J. Chem. Sci. Vol. 129, No. 2, February 2017, pp. 149–156.
DOI 10.1007/s12039-017-1221-6

RAPID COMMUNICATION

1,6-Diaminoperylene bisimide with a highly twisted perylene core

CHE-WEI CHANG, FANG-YUN CHIEN, JIUN-WEI HU, HSING-YANG TSAI and KEW-YU CHEN*

Department of Chemical Engineering, Feng Chia University, 40724 Taichung, Taiwan, Republic of China
Email: kyuchen@fcu.edu.tw

MS received 27 July 2016; revised 22 September 2016; accepted 3 January 2017

Abstract. 1,6-Diaminoperylene bisimide (**1**) was synthesized and characterized by single-crystal X-ray diffraction. To the best of our knowledge, this is the first time that the structure of 1,6-disubstituted perylene bisimide has been reported. The crystal belongs to triclinic, space group P-1, with $a = 10.3966(10)$, $b = 15.3398(16)$, $c = 16.8495(17)$ Å, $\alpha = 79.490(4)°$, $\beta = 87.055(3)°$, $\gamma = 79.423(3)°$, and Z = 2. Compound **1** possesses two intramolecular C–H···N hydrogen bonds, which generate two S(6) ring motifs. The central perylene core of **1** is twisted with dihedral angles of 19.48(2)° and 19.50(2)°; this twist configuration induces the axial chirality in this family of perylene bisimide chromophores. Density functional theory (DFT) calculations also show that the core twist angles of 1,6-diaminoperylene bisimide are larger than those of 1,7-diaminoperylene bisimide, which may account for the fact that the 1,7-regioisomer has a more extended effective conjugation length than the 1,6-regioisomer.

Keywords. Perylene bisimides; x-ray diffraction; axial chirality; density functional theory.

1. Introduction

Perylene bisimides (PBIs) and their derivatives have attracted an increasing interest due to their potential applications in molecular optoelectronic devices, such as LCD color filters,[1] light-emitting diodes,[2] photovoltaic cells,[3,4] light-harvesting arrays,[5] photochromic materials,[6] and organic field-effect transistors (OFETs).[7] This family of organic chromophores is advantageous due to their large electron mobility, high photoluminescence quantum yields and molar absorptivities, excellent thermal and optical stabilities, reversible redox properties, self-assembly behaviors, and ease of synthetic modification.[8–30] To date, a useful method for introducing substituents onto the PBIs core is bromination or chlorination of perylene-3,4,9,10-tetracarboxylic dianhydride. Nucleophilic substitutions and metal-catalyzed cross-coupling reactions can then be performed which yield a regioisomeric mixture of 1,6- and 1,7-disubstituted PBIs. However, only a few reports of isolation and characterization of both 1,6- and 1,7-disubstituted PBIs have been reported, and still very little is known about the molecular structures and spectroscopic properties of 1,6-disubstituted PBIs.[31–33] To reveal the structure-property relationship of PBI molecules, we herein report the single-crystal X-ray diffraction structure and complementary density functional theory (DFT) calculations of 1,6-diaminoperylene bisimide (**1**). The results offer the potential to synthesize 1,6-disubstituted PBIs with extended molecular architectures and photophysical properties.

2. Experimental

2.1 *Chemicals and instruments*

The starting materials, such as 3,4,9,10-perylenetetracarboxylic dianhydride, acetic acid, cyclohexylamine, cerium (IV) ammonium nitrate (CAN), tin(II) chloride dihydrate ($SnCl_2.2H_2O$), sodium hydride (NaH), 1-iodohexane ($C_6H_{13}I$), tetrahydrofuran (THF), and *N*-methyl-2-pyrrolidinone (NMP) were purchased from Merck, ACROS and Sigma–Aldrich. Column chromatography was performed using silica gel Merck Kieselgel *si* 60 (40–63 mesh).

^1H and ^{13}C NMR spectra were recorded in $CDCl_3$ on a Bruker 400 MHz. Mass spectra were recorded on a VG70-250S mass spectrometer. The absorption and emission spectra were measured using a Jasco V-570 UV–Vis spectrophotometer and a Hitachi F-7000 fluorescence spectrophotometer, respectively. Cyclic voltammetry (CV) was performed with a CH instruments at a potential scan rate of 200 mV/s in a 0.1 M solution of tetrabutylammonium hexafluorophosphate ($TBAPF_6$) in dichloromethane. Platinum and $Ag/AgNO_3$ electrodes were used as counter and reference electrodes, respectively. The single crystal X-ray diffraction data were collected on a Bruker Smart 1000CCD area-detector diffractometer.

*For correspondence

2.2 *Synthesis and characterization*

2.2a *Synthesis of **5** and **6***: Compound **7** (1.0 g, 1.8 mmol), CAN (4.8 g, 8.8 mmol), nitric acid (8.0 g, 131.1 mmol) and dichloromethane (250 mL) were stirred at 25°C under N_2 for 48 h. The mixture was neutralized with 10% KOH and extracted with CH_2Cl_2. After the solvent was removed, the crude product was purified by silica gel column chromatography with eluent CH_2Cl_2 to afford a mixture of 1,6- and 1,7-dinitroperylene bisimides, and ^{1}H-NMR (400 MHz) analysis revealed a 1:3 ratio. Separation of the 1,6 and 1,7 isomers was performed on a preparative HPLC system equipped with a refractive index detector and fitted with a macro-HPLC column (Si, 8 μm, 250 × 22 mm). The eluent was 8:1 hexane/ethyl acetate flowing at 12 mL/min. Two fractions were collected from the column; the first was pure 1,6-isomer (R_f = 0.42, 242 mg, yield = 21%), and the second was pure 1,7-isomer (R_f = 0.38, 682 mg, yield = 59%). Characterization data: **5**: ^{1}H NMR (400 MHz, $CDCl_3$) δ 8.78 (2H, s), 8.63 (2H, d, J = 8.0 Hz), 8.30 (2H, d, J = 8.0 Hz), 5.01 (2H, m), 2.52 (4H, m), 1.90 (4H, m), 1.74 (6H, m), 1.46 (4H, m), 1.36 (2H, m); MS (FAB): m/z (relative intensity) 645 [M+H$^+$, 100]; HRMS calcd. for $C_{36}H_{29}O_8N_4$ 645.1985, found 645.1983. Selected data for **6**: ^{1}H NMR (400 MHz, $CDCl_3$) δ 8.78 (2H, s), 8.68 (2H, d, J = 8.4 Hz), 8.28 (2H, d, J = 8.4 Hz), 5.01 (2H, m), 2.51 (4H, m), 1.92 (4H, m), 1.74 (6H, m), 1.46 (4H, m), 1.36 (2H, m); MS (FAB): m/z (relative intensity) 645 [M+H$^+$, 100]; HRMS calcd. for $C_{36}H_{29}O_8N_4$ 645.1985, found 645.1977.

2.2b *Synthesis of **3** and **4***: Tin(II) chloride dihydrate (1.0 g, 4.8 mmol), 1,6- or 1,7-dinitroperylene diimides (0.5 g, 0.8 mmol) were suspended in THF (50 mL), and stirred at 25°C under N_2 for 20 min. The solvent was refluxed 80°C with stirring for 6 h. THF was removed at the rotary evaporator, and the residue was dissolved in ethyl acetate and washed with 10% sodium hydroxide solution and brine. The organic layer was dried over anhydrous $MgSO_4$ and the filtrate was concentrated under reduced pressure. The crude product was purified by silica gel column chromatography with eluent ethyl acetate/*n*-hexane (4/5) to afford **3** (**4**) in 80% (82%) yield. Characterization data: **3**: ^{1}H NMR (400 MHz, $CDCl_3$) δ 8.77 (2H, d, J = 8.0 Hz), 8.51 (2H, d, J = 8.0 Hz), 7.85 (2H, s), 5.05 (2H, m), 4.98 (4H, s), 2.59 (4H, m), 1.92 (4H, m), 1.76 (6H, m), 1.27–1.56 (6H, m); MS (FAB): m/z (relative intensity) 585 [M+H$^+$, 100]; HRMS calcd. for $C_{36}H_{33}O_4N_4$ 585.2502, found 585. 2508. Selected data for **4**: ^{1}H NMR (400 MHz, $CDCl_3$) δ 8.90 (2H, d, J = 8.0 Hz), 8.25 (2H, d, J = 8.0 Hz), 8.14 (2H, s), 5.04, (2H, m), 4.94 (4H, s), 2.61 (4H, m), 1.93 (4H, m), 1.74 (6H, m), 1.36–1.54 (6H, m); MS (FAB): m/z (relative intensity) 585 (M+H$^+$, 100); HRMS calcd. for $C_{36}H_{33}O_4N_4$ 585.2502, found 585.2504.

2.2c *Synthesis of **1** and **2***: A mixture of solution of **3** or **4** (410 mg, 0.70 mmol), sodium hydride (97%, 200 mg, 8.00 mmol) and dry THF (25 mL) was stirred at 0°C under N_2 for 30 min. 1-iodohexane (890 mg, 4.20 mmol) was then added and the resulting mixture was stirred for 6 h. The resulting mixture was diluted with 75 mL of water and extracted with CH_2Cl_2. The crude product was purified by silica gel column chromatography with eluent ethyl acetate/n-hexane (1/2) to afford **1** (**2**) in 85% (82%) yield. Characterization data for **1**: ^{1}H NMR (400 MHz, $CDCl_3$) δ 9.40 (d, J = 8.0 Hz, 2H), 8.55 (d, J = 8.0 Hz, 2H), 8.32 (s, 2H), 5.06, (m, 2H), 3.35 (m, 4H), 3.01 (m, 4H), 2.57 (m, 4H), 1.90 (m, 4H), 1.15–1.77 (m, 44H), 0.78 (t, J = 6.4 Hz, 12H); ^{13}C NMR (100 MHz, $CDCl_3$) δ 164.5, 164.3, 151.0, 135.8, 131.9, 130.9, 128.9, 128.0, 123.7, 123.2, 123.1, 123.0, 120.3, 54.0, 53.6, 52.8, 31.5, 29.2, 29.1, 27.3, 26.9, 26.6, 25.5, 22.5, 13.9; MS (FAB): m/z (relative intensity) 921 (M+H$^+$, 100); HRMS calcd. for $C_{60}H_{81}O_4N_4$ 921.6256, found 921.6247. Purple parallelepiped-shaped crystals suitable for the crystallographic studies reported here were isolated over a period of six weeks by slow evaporation from a dichloromethane solution. Selected data for **2**: ^{1}H NMR (400 MHz, $CDCl_3$) δ 9.21 (d, J = 8.0 Hz, 2H), 8.45 (s, 2H), 8.38 (d, J = 8.0 Hz, 2H), 5.03, (m, 2H), 3.45 (m, 4H), 3.15 (m, 4H), 2.57 (m, 4H), 1.87 (m, 4H), 1.15–1.75 (m, 44H), 0.82 (t, J = 6.4 Hz, 12H); ^{13}C NMR (100 MHz, $CDCl_3$) δ 164.5, 164.2, 148.5, 135.4, 130.3, 128.2, 125.3, 124.3, 122.9, 122.7, 122.6, 121.1, 53.8, 52.5, 31.4, 29.1, 27.5, 26.9, 26.6, 25.5, 22.5, 13.9; MS (FAB): m/z (relative intensity) 921 (M+H$^+$, 100); HRMS calcd. for $C_{60}H_{81}O_4N_4$ 921.6256, found 921.6250.

2.2d *Crystal structural determination*: A single crystal of **1** with dimensions of 0.35 mm × 0.33 mm × 0.08 mm was selected. The lattice constants and diffraction intensities were measured with a Bruker Smart 1000CCD area detector radiation (λ = 0.71073 Å) at 156(2) K. An ω-2θ scan mode was used for data collection in the range of $3.02 \leq \theta \leq 26.45°$. A total of 77973 reflections were collected and 10645 were independent (R_{int} = 0.0595), of which 6504 were considered to be observed with $I > 2\sigma(I)$ and used in the succeeding refinement. The structure was solved by direct methods with SHELXS-97[34] and refined on F^2 by full-matrix least-squares procedure with Bruker SHELXL-97 packing.[35] All non-hydrogen atoms were refined with anisotropic thermal parameters. The hydrogen atoms refined with riding model position parameters isotropically were located from difference Fourier map and added theoretically. At the final cycle of refinement, R = 0.1001 and wR = 0.2669 ($w = 1/[\sigma^2(F_o^2) + (0.1983P)^2 + 2.9730P]$, where $P = (F_o^2 + 2F_c^2)/3$). S = 1.078, $(\Delta/\sigma)_{max}$ = 0.001, $(\Delta/\rho)_{max}$ = 0.726 and $(\Delta/\rho)_{min} = -1.159$ e/Å^3. Crystallographic data for the structural reported in this article have been deposited with the Cambridge Crystallographic Data Center as supplementary publication number CCDC 1486032. Copies of these information can be obtained free of charge from the Director, CCDC, 12 Union Road, Cambridge CB2 1EZ, UK (fax: +44 1223 336 033; e-mail: deposit@ccdc.cam.ac.uk).

2.3 *Computational methods*

The Gaussian 03 program was used to perform the ab initio calculation on the molecular structure.[36] Geometry

optimizations for 1,6-diaminoperylene bisimide (**1**) and 1,7-diaminoperylene bisimide (**2**) were carried out with the 6-31G* basis set to the B3LYP functional. Vibrational frequencies were also performed to check whether the optimized geometrical structures for both compounds were at energy minima, transition states, or higher order saddle points. After obtaining the converged geometries, the TD-B3LYP/6-31G* was used to calculate the vertical excitation energies.

3. Results and Discussion

Scheme 1 shows the chemical structure and the synthetic route of **1**. In brief, the synthesis of **1** started from a dinitration of perylene bisimide (**7**), giving 1,6- and 1,7-dinitroperylene bisimides (**5** and **6**).[26,31] The regioisomeric 1,6- and 1,7-dinitroperylene bisimides can be separated by high performance liquid chromatography (HPLC). Next, the reduction of 1,6-dinitroperylene bisimide (**5**) by tin(II) chloride dihydrate ($SnCl_2 \cdot 2H_2O$) gave 1,6-diaminoperylene bisimide (**3**). Finally, 1,6-dialkylamino-substituted perylene bisimide (**1**) was synthesized by the alkylation of **3** with 1-iodohexane. To confirm its structure, a single crystal of **1** was obtained from a dichloromethane solution, and the molecular structure was determined by X-ray diffraction analysis. Additionally, its X-ray structure is compared with that of other PBI derivatives.[27,29]

Figure 1 shows the ORTEP (Oak Ridge Thermal Ellipsoid Plot) diagram of **1** and the numbering of the atoms. Compound **1** crystallizes in the triclinic space group P-1, with $a = 10.3966(10)$, $b = 15.3398(16)$,

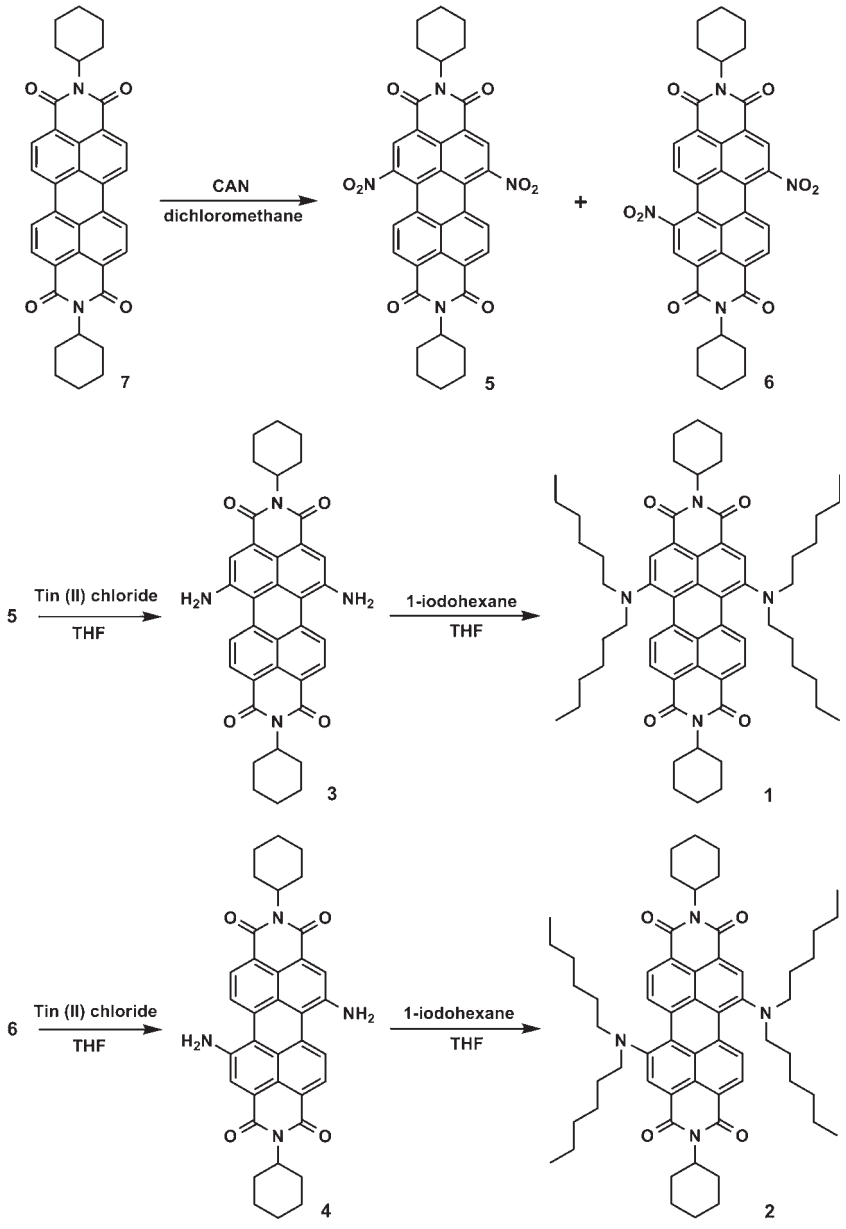

Scheme 1. The synthetic routes for **1** and **2**.

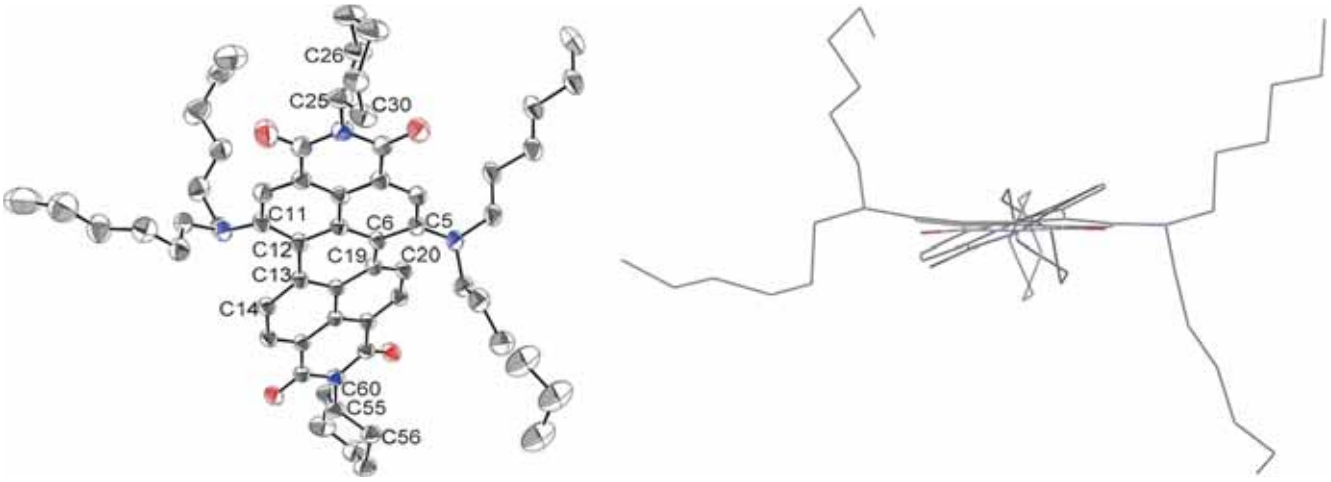

Figure 1. Molecular structure of **1** (left) and viewed along the N–N axis showing the twisted perylene backbone (right, all hydrogen atoms are omitted for clarity). Displacement ellipsoids are drawn at the 50% probability level.

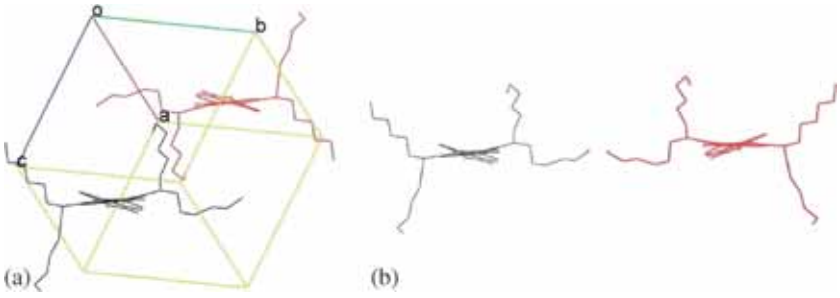

Figure 2. (a) Crystal structure of **1** in the unit cell. (b) The black-colored molecule is the *M* enantiomer and the red-colored one is the *P* enantiomer. For clarity, only the PBI scaffold and the alkyl amino groups are shown.

$c = 16.8495(17)$ Å, $\alpha = 79.490(4)°$, $\beta = 87.055(3)°$, $\gamma = 79.423(3)°$, and $Z = 2$. The central perylene core of **1** is twisted with dihedral angles of 19.48(2)° and 19.50(2)° associated with bay area carbon atoms C11–C12–C13–C14 and C5–C6–C19–C20, respectively, these values being larger than those of unsubstituted and mono-substituted PBIs.[30] This twist configuration also induces the axial chirality in this family of PBI chromophores. As shown in Figure 2, there are two molecules with opposite chirality in the unit cell. Nevertheless, the enantiomers are only observed in the crystalline state due to the low barrier of rotation in solution. Furthermore, all C–C bond lengths of the perylene backbone range between 1.363 and 1.480 Å, which indicates the presence of π-conjugation for all C–C bonds. The longest bonds in the perylene moiety are the C6–C19 and C12–C13 bonds that connect the two naphthalene rings at a distance of ~1.47 Å. The bond length is slightly different to the lengths observed for other PBIs.[27,29,30] The results show that the degree of conjugation of the perylene scaffold is similar but different in unsubstituted and core-substituted PBIs.

Compound **1** possesses two intramolecular C–H···N hydrogen bonds (Table 1), which generate two S(6) ring motifs (red dashed lines in Figure 3). In good agreement with this observation, the ^{1}H NMR spectrum (in $CDCl_3$) revealed a significantly downfield signal at δ 9.38 ppm (H14A and H20A), giving a clear indication of the six-membered ring intramolecular hydrogen bonds formation. The molecule is further stabilized by six different intramolecular C–H···O hydrogen bonds (green dashed lines in Figure 3 and Table 1). In addition, intermolecular C–H···π interactions (2.82 Å of H(60A)···*Cg*1 distance and 115° of C(60)–H(60A)–*Cg*1, symmetry code: –X, 1–Y, 2–Z) is also observed in the crystal structure (blue dashed lines in Figure 3), which links a pair of molecules into a cyclic centrosymmetric dimer. Careful examination of the crystal structure also shows that there is no substantial π–π stacking between the perylene plane and its adjacent one. As a result, we can ascertain that the bulky *n*-hexyl groups not only largely increase the solubility of **1** compared with **3**, but also reduce intermolecular contact and aggregation.

Table 1. Hydrogen-bond geometry (Å, °).

D–H···A	d(D–H)	d(H···A)	d(D···A)	∠DHA
C(14)–H(14A)···N(3)	0.95	2.37	2.916(4)	116.0(3)
C(20)–H(20A)···N(2)	0.95	2.35	2.907(4)	116.7(6)
C(25)–H(25A)···O(1)	1.00	2.11	2.661(16)	112.6(7)
C(26)–H(26B)···O(2)	0.99	2.51	3.067(7)	115.0(3)
C(30)–H(30B)···O(2)	0.99	2.56	3.112(18)	115.1(4)
C(55)–H(55A)···O(4)	1.00	2.22	2.717(5)	109.3(4)
C(56)–H(56B)···O(3)	0.99	2.38	2.955(5)	116.4(6)
C(60)–H(60A)···O(3)	0.99	2.58	3.116(5)	113.9(7)

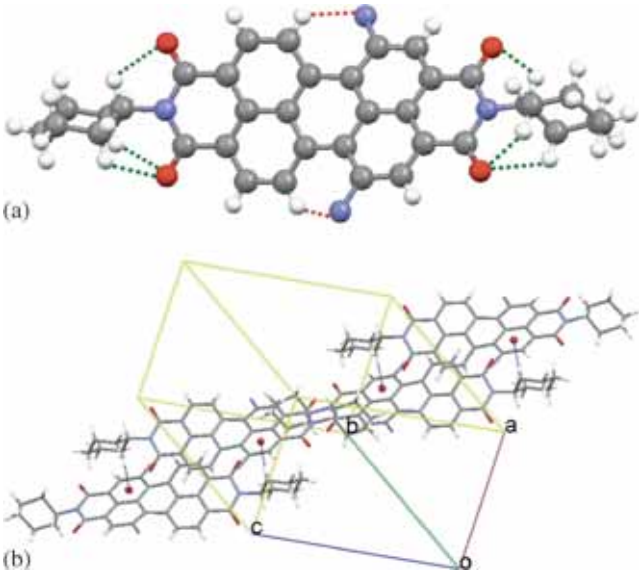

Figure 3. (a) Crystal structure of **1**. Red and Green dashed lines denote intramolecular C–H···N and C–H···O hydrogen bonds, respectively. (b) A packing view of **1**. Blue dashed lines denote intermolecular C–H···π interactions. *Cg*1 (red circles) is the centroid of the C3–C8 ring. Hexyl groups are omitted for clarity.

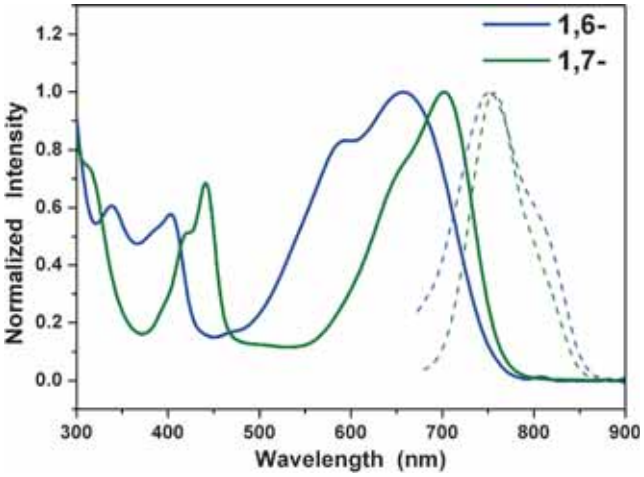

Figure 4. Normalized absorption (solid lines) and emission (dashed lines) spectra of **1** (1,6-isomer) and **2** (1,7-isomer) in dichloromethane.

Figure 4 shows the steady state absorption and emission spectra of 1,6-diaminoperylene bisimide (**1**) and 1,7-diaminoperylene bisimide (**2**) in dichloromethane. The absorption spectra of both regioisomers are dominated by very broad absorption bands that cover a large part of the visible spectrum (300–800 nm). These broad bands are typical for perylene bisimide derivatives *N*-substituted at the bay-core positions, due to charge transfer absorption.[16] The 1,6- and 1,7-regioisomers show significant differences in their optical characteristics. In addition to the longest wavelength absorption band at around 657 nm, **1** exhibits another shoulder band at *ca.* 595 nm, and consequently, cover a large part of the visible region relative to that of 1,7-diaminoperylene bisimide (**2**). Interestingly, the longest wavelength absorption band (702 nm) of **2** (1,7-) is 45 nm red-shifted relative to that of **1** (1,6-), which can be explained by the fact that the 1,7-regioisomer has a more extended effective conjugation length than **1**. As for the steady-state emission, both compounds emit in the near-infrared region (>700 nm). As a result, the 1,6-regioisomer may be of particular interest for organic photovoltaic and near-infrared fluorescent dye applications.

To gain more insight into the molecular structures of 1,6-diaminoperylene bisimide (**1**) and 1,7-diaminoperylene bisimide (**2**), quantum mechanical calculations were performed using density functional theory (DFT) at the B3LYP/6-31G* level. DFT calculations show that the ground-state geometries of the perylene core have different core twist angles (Figure 5), *i.e.*, approximate dihedral angles between the two naphthalene subunits attached to the central benzene ring; these are ∼19.0° and ∼19.1° for **1** (1,6-) and ∼17.6° and ∼17.7° for **2** (1,7-). The core twist angles of 1,6-disubstituted PBI are slightly larger than those of 1,7-disubstituted PBI. The results may account for the fact that the 1,7-regioisomer has a more extended effective conjugation length than the 1,6-regioisomer.[32,33]

Figure 6 shows the highest occupied molecular orbitals (HOMOs) and the lowest unoccupied molecular orbitals (LUMOs) of **1** and **2**. The HOMO of both

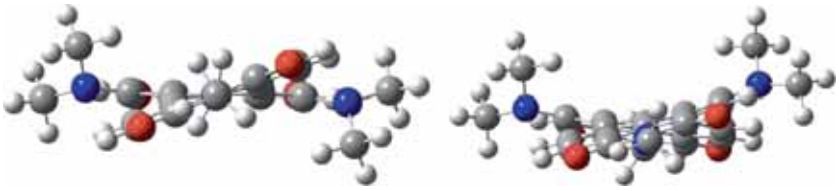

Figure 5. DFT (B3LYP/6-31G*) geometry-optimized structures of **1** (left) and **2** (right) shown with view along the long perylene axis. For computational purposes, methyl groups replace the cyclohexyl and hexyl groups.

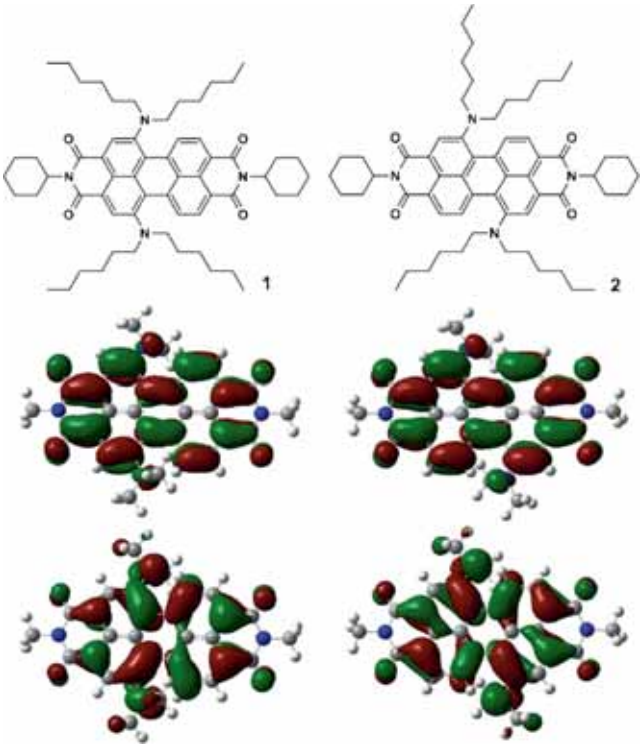

Figure 6. Calculated frontier orbitals for **1** and **2**. The upper structures show the LUMOs and the lower ones show the HOMOs. Methyl groups replace the cyclohexyl and hexyl groups for clarity.

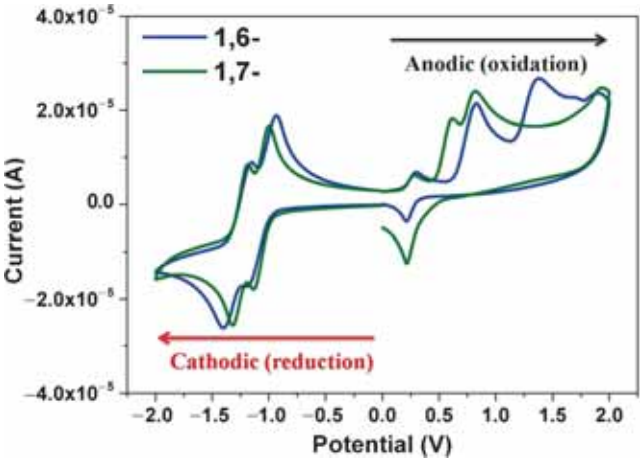

Figure 7. The cyclic voltammograms of **1** and **2** measured in dichloromethane solution (versus SCE) with ferrocenium/ferrocene as an internal standard, at 200 mV/s.

compounds is delocalized mainly on the amino group and the perylene core, while the LUMO is extended from the central perylene core to the bisimide groups. Furthermore, the absorption spectra of **1** and **2** were calculated by time-dependent DFT (TD-DFT) calculations (Franck–Condon principle). The calculated excitation wavelengths for **1** and **2** are 624 (oscillator strength: $f = 0.3530$) and 643 ($f = 0.3758$) nm, respectively, which are in good agreement with the experimental results.

The cyclic voltammograms of 1,6- and 1,7-diaminoperylene bisimides (**1** and **2**) are shown in Figure 7. Both compounds exhibit two irreversible one-electron oxidations and two quasi-reversible one-electron reductions in dichloromethane. The one-electron oxidation of **2** occurs at 0.62 V, whereas for **1**, the first oxidation is shifted to more positive values by 0.21 V. The results clearly show that the removal of one electron from **1** (1,6-) is more difficult in comparison to **2** (1,7-); these findings are in good agreement with previous reports.[31]

4. Conclusions

1,6−diaminoperylene bisimide (**1**) was synthesized and characterized by single crystal X-ray diffraction. Compound **1** crystallizes in the triclinic space group P-1 and possesses two intramolecular C–H$\cdots$N hydrogen bonds with two S(6) graph-set motifs. The core twist angles of **1** are much larger than those of unsubstituted and mono-substituted PBIs. DFT calculations also showed that the core twist angles of 1,6-disubstituted PBI are slightly larger than those of 1,7-disubstituted PBI, which may account for the fact that the 1,7-regioisomer has a smaller band gap than the 1,6-regioisomer. This twist configuration induces the axial chirality in this family of PBI chromophores; the two enantiomers are only observed in the crystalline state due to the low barrier of rotation in solution. Moreover, the crystal structure is stabilized by intermolecular C–H$\cdots\pi$ hydrogen bonds rather than $\pi-\pi$ interactions, which indicates that the bulky n-hexyl groups not

only largely increase the solubility of **1** compared with **3**, but also reduce intermolecular contact and aggregation. This offers the potential for synthesizing PBI derivatives with extended molecular architectures and optical properties.

Supplementary Information (SI)

Supplementary Information (^{1}H and ^{13}C NMR spectra) is available at www.ias.ac.in/chemsci.

Acknowledgements

The project was supported by the Ministry of Science and Technology (MOST 105-2113-M-035-001).

References

1. Liang Y, Wang H, Wang D, Liu H and Feng S 2012 The synthesis, morphology and liquid-crystalline property of polysiloxane-modified perylene derivative *Dyes Pigm.* **95** 260
2. Daimon T and Nihei E 2013 Fabrication of a poly(3-octylthiophene-2,5-diyl) electrochemiluminescence device assisted by perylene *Materials* **6** 1704
3. Kozma E and Catellani M 2013 Perylene diimides based materials for organic solar cells *Dyes Pigm.* **98** 160
4. Kozma E, Kotowski D, Catellani M, Luzzati S, Famulari A and Bertini F 2013 Synthesis and characterization of new electron acceptor perylene diimide molecules for photovoltaic applications *Dyes Pigm.* **99** 329
5. Chang C W, Tsai H Y and Chen K Y 2014 Green perylene bisimide dyes: Synthesis, photophysical and electrochemical properties *Materials* **7** 5488
6. Tan W, Li X, Zhang J and Tian H 2011 A photochromic diarylethene dyad based on perylene diimide *Dyes Pigm.* **89** 260
7. Chen K Y and Chow T J 2010 1,7-Dinitroperylene bisimides: Facile synthesis and characterization as *n*-type organic semiconductors *Tetrahedron Lett.* **51** 5959
8. Han M, Wang G C and Duan H Q 2014 Construction of supramolecular nanofibers through electrostatic interaction between perylene and cholesterol derivatives *Chin. Chem. Lett.* **25** 51
9. Wei Z J, Xu Y W, Zhang L and Luo M M 2014 Synthesis and thermal polymerization of perylene bisimide containing benzocyclobutene groups *Chin. Chem. Lett.* **25** 1367
10. Singh M K and Bandyopadhyay D 2016 Design and synthesis of nanoporous perylene bisimide linked metalloporphyrin frameworks and their catalytic activity *J. Chem. Sci.* **128** 1
11. Divya K P, Bertocchi M J and Weiss R G 2016 Effects of temperature and CO_2 pressure on the emission of N,N′-dialkylated perylene diimides in poly(alkyl methacrylate) films. Are guest-host alkyl group interactions important? *J. Chem. Sci.* **128** 119
12. Damaceanu M D, Constantin C P, Bruma N and Pinteala M 2013 Tuning of the color of the emitted light from new polyperyleneimides containing oxadiazole and siloxane moieties *Dyes Pigm.* **99** 228
13. Li J, Yu X, Fu J, Liu X and Zeng Y 2010 A novel perylene diimide-based tetrahedral molecule: Synthesis, characterization and self-assembly with gold nanoparticles *J. Chem. Sci.* **122** 839
14. Ramanan C, Semigh A L, Anthony J E, Marks T J and Wasielewski M R 2012 Competition between singlet fission and charge separation in solution-processed blend films of 6,13-bis(triisopropylsilylethynyl)-pentacene with sterically-encumbered perylene-3,4:9,10-bis(dicarboximide)s *J. Am. Chem. Soc.* **134** 386
15. Lucenti E, Botta C, Cariati E, Righetto S, Scarpellini M, Tordin E and Ugo R 2013 New organic-inorganic hybrid materials based on perylene diimide–polyhedral oligomeric silsesquioxane dyes with reduced quenching of the emission in the solid state *Dyes Pigm.* **96** 748
16. Ahrens M J, Tauber M J and Wasielewski M R 2006 Bis(n-octylamino)perylene-3,4:9,10-bis(dicarboximide)s and their radical cations: Synthesis, electrochemistry, and ENDOR spectroscopy *J. Org. Chem.* **71** 2107
17. Langhals H and Kirner S 2000 Novel fluorescent dyes by the extension of the core of perylenetetracarboxylic bisimides *Eur. J. Org. Chem.* **2** 365
18. Wilson T M, Tauber M J and Wasielewski M R 2009 Toward an *n*-type molecular wire: Electron hopping within linearly linked perylenediimide oligomers *J. Am. Chem. Soc.* **131** 8952
19. Kang H, Jiang W and Wang Z 2013 Construction of well-defined butadiynylene-linked perylene bisimide arrays *via* cross-coupling *Dyes Pigm.* **97** 244
20. Zhao C, Zhang Y, Li R, Li X and Jiang J 2007 Di(alkoxy)- and di(alkylthio)-substituted perylene-3,4;9,10-tetracarboxy diimides with tunable electrochemical and photophysical properties *J. Org. Chem.* **72** 2402
21. Zhang X, Pang S, Zhang Z, Ding X, Zhang S, He S and Zhan C 2012 Facile synthesis of 1-bromo-7-alkoxyl perylene diimide dyes: Toward unsymmetrical functionalizations at the 1,7-positions *Tetrahedron Lett.* **53** 1094
22. Sengupta S, Dubey R K, Hoek R W M, van Eeden S P P, Gunbaş D D, Grozema F C, Sudhölter E J R and Jager W F 2014 Synthesis of regioisomerically pure 1,7-dibromoperylene-3,4,9,10-tetracarboxylic acid derivatives *J. Org. Chem.* **79** 6655
23. Wang R, Shi Z, Zhang C, Zhang A, Chen J, Guo W and Sun Z 2013 Facile synthesis and controllable bromination of asymmetrical intermediates of perylene monoanhydride/monoimide diester *Dyes Pigm.* **98** 450
24. Chen K Y, Fang T C and Chang M J 2011 Synthesis, photophysical and electrochemical properties of 1-aminoperylene bisimides *Dyes Pigm.* **92** 517
25. Tsai H Y and Chen K Y 2013 1,7-Diaminoperylene bisimides: Synthesis, optical and electrochemical properties *Dyes Pigm.* **96** 319
26. Chen K Y and Chang C W 2014 1,7-Bis-(*N*,*N*-dialkylamino)perylene bisimides: Facile synthesis and characterization as near-infrared fluorescent dyes *Materials* **7** 7548
27. Luo M H and Chen K Y 2013 Asymmetric perylene bisimide dyes with strong solvatofluorism *Dyes Pigm.* **99** 456
28. Tsai H Y and Chen K Y 2014 Synthesis and optical properties of novel asymmetric perylene bisimides *J. Lumin.* **149** 103

29. Chen K Y and Chang C W 2014 Highly soluble monoamino-substituted perylene tetracarboxylic dianhydrides: Synthesis, optical and electrochemical properties *Int. J. Mol. Sci.* **15** 22642
30. Chang C W and Chen K Y 2016 Crystal structure of *N*,*N*′-bis(cyclohexyl)-1-(*N*,*N*-dihexylamino)perylene-3,4:9,10-bis(dicarboximide) *Mol. Cryst. Liquid Cryst.* **624** 205
31. Tsai H Y, Chang C W and Chen K Y 2014 1,6- And 1,7-regioisomers of dinitro- and diamino-substituted perylene bisimides: Synthesis, photophysical and electrochemical properties *Tetrahedron Lett.* **55** 884
32. Chen K Y, Chang C W and Tsai H Y 2015 1,6- And 1,7-Regioisomers of Highly Soluble Amino-Substituted Perylene Tetracarboxylic Dianhydrides: Synthesis, Optical and Electrochemical Properties *Materials* **8** 4943
33. Tsai H Y, Chang C W and Chen K Y 2014 1,6- and 1,7-Regioisomers of asymmetric and symmetric perylene bisimides: Synthesis, characterization and optical properties *Molecules* **19** 327
34. Sheldrick G M 1997 In *SHELXS97, A Program for Automatic Solution of Crystal Structure* (Germany: University of Göttingen)
35. Sheldrick G M 1997 In *SHELX97*, *A Program for Crystal Structure Refinement* (Germany: University of Göttingen)
36. Frisch M J, Trucks G W, Schlegel H B, Scuseria G E, Robb M A, Cheeseman J R, Montgomery J A, Jr. Vreven T, Kudin K N, Burant J C, Millam J M, Iyengar S S, Tomasi J, Barone V, Mennucci B, Cossi M, Scalmani B, Rega G N, Petersson G A, Nakatsuji H, Hada M, Ehara M, Toyota K, Fukuda R, Hasegawa J, Ishida M, Nakajima T, Honda Y, Kitao O, Nakai H, Klene M, Li X, Knox J E, Hratchian H P, Cross J B, Adamo C, Jaramillo J, Gomperts R, Stratmann R E, Yazyev O, Austin A J, Cammi R, Pomelli C, Ochterski J W, Ayala P Y, Morokuma K, Voth G A, Salvador P, Dannenberg J J, Zakrzewski V G, Dapprich S, Daniels A D, Strain M C, Farkas O, Malick D K, Rabuck A D, Raghavachari K, Foresman J B, Ortiz J V, Cui Q, Baboul A G, Clifford S, Cioslowski J, Stefanov B B, Liu G, Liashenko A, Piskorz P, Komaromi I, Martin R L, Fox D J, Keith T, Al-Laham M A, Peng C Y, Nanayakkara A, Challacombe M, Gill P M W, Johnson B, Chen W, Wong M W, Gonzalez C and Pople J A 2003 Gaussian, Inc., Pittsburgh PA